Smart Structures and Systems, *Vol. 24, No. 1 (2019) 1-14*
DOI: https://doi.org/10.12989/sss.2019.24.1.001

Temperature effect on seismic behavior of transmission tower-line system equipped with SMA-TMD

Li Tian[1], Juncai Liu[1], Canxing Qiu[*2] and Kunjie Rong[1]

[1]*School of Civil Engineering, Shandong University, No. 17922 Jingshi Road, Jinan, Shandong 250061, China*
[2]*Key Laboratory of Urban Security and Disaster Engineering of Ministry of Education, Beijing University of Technology, Beijing 100124, China*

(Received February 28, 2019, Revised March 8, 2019, Accepted March 10, 2019)

Abstract. Transmission tower-line system is one of most critical lifeline systems to cities. However, it is found that the transmission tower-line system is prone to be damaged by earthquakes in past decades. To mitigate seismic demands, this study introduces a tuned-mass damper (TMD) using superelastic shape memory alloy (SMA) spring for the system. In addition, considering the dynamic characteristics of both tower-line system and SMA are affected by temperature change. Particular attention is paid on the effect of temperature variation on seismic behavior. In doing so, the SMA-TMD is installed into the system, and its properties are optimized through parametric analyses. The considered temperature range is from -40 to 40℃. The seismic control effect of using SMA-TMD is investigated under the considered temperatures. Interested seismic performance indices include peak displacement and peak acceleration at the tower top and the height-wise deformation. Parametric analyses on seismic intensity and frequency ratio were carried out as well. This study indicates that the nonlinear behavior of SMA-TMD is critical to the control effect, and proper tuning before application is advisable. Seismic demand mitigation is always achieved in this wide temperature range, and the control effect is increased at high temperatures.

Keywords: SMA-TMD; temperature effect; transmission tower-line system; vibration control; seismic analysis

1. Introduction

Power transmission tower-line system is one of major components of the lifeline systems. The seismic safety during earthquakes of such system is critical to the post-earthquake recovery of the attacked regions, but the damage cases of the tower-line systems can be found in many scenarios during past years. For example, in the 1994 Northridge earthquake (Hall and Holmes 1994), several transmission towers collapsed, which lead to power cut off in a large area of the city and long-time interruptions of daily lives. In the year of 2014, a total of 36 transmission towers were seriously damaged by the earthquake occurred in Yunnan of China (Shuai 2014), which also caused huge lost to the affected regions. Thus, there is a pressing need to well control the seismic demands for transmission tower-line systems, with the purpose of maintaining their normal operation after earthquakes.

In recognition of the damage risk due to earthquakes, great efforts were paid on seismic control strategy for transmission tower-line systems. Kilroe (2000) installed dampers on the affected members of the transmission towers to solve the fatigue problem of the towers caused by external loads. Wu (2011) studied the influence of tower-line coupling effect on the performance of TMD under earthquakes. It is concluded that the tower-line coupling effect affects the performance of TMD significantly in the transmission tower-line system. Zhang (2012) combined traditional TMD and energy-dissipating materials and proposed a pounding tuned mass damper (PTMD). Comparison between traditional TMD and the PTMD showed that the vibration reduction effect of PTMD is better than that of traditional TMD. Tian (2013) presented equations of motion of transmission tower-line system with TMD under multi-component ground motion excitations and optimized the design of the TMD damper according to the mass ratio. Miguel (2016) used backtracking search optimization algorithm to determine optimal friction forces and the location of friction dampers in structures, and studied the vibration response of the tower-line system under earthquake ground motions. The results showed that the vibration reduction effect of the optimized friction dampers is the best among all cases. Chen (2017) developed an approach for assessing energy response of the transmission tower- line system with friction dampers subjected to seismic excitations, and carried out the dynamic response analysis. Numerical results demonstrated that the best control performance of a transmission tower can be achieved by optimizing friction damper parameters. However, it is worth noting that the tower-line systems usually operate in outdoor environment, which is subjected to severe temperature variation. Due to temperature change, the stress state and stiffness in transmission lines will be varied, which lead to varied dynamic characteristics consequently. But the issue associated with temperature change was selfdom considered in prior studies. Thus, it is necessary to include the temperature effect in the seismic

*Corresponding author, Professor
E-mail: qiucanxing@bjut.edu.cn

http://www.techno-press.com/journals/sss&subpage=7
ISSN: 1738-1584 (Print), 1738-1991 (Online)

Table 1 Performance indices of the transmission lines

Parameters	Conductor wire	Ground wire
Type	LGJ-400/35	LGJ-95/55
Outer diameter (mm)	26.82	16
Cross-sectional area (mm^2)	425.24	152.81
Elastic modulus (GPa)	65	105
Mass per unit length (kg/m)	1.349	0.7077
Density (kg/m^3)	3172.326	4631.241
Coefficient of linear expansion ($1/^oC$)	2.05E-005	1.55E-005

control problem of transmission tower-line systems.

Recent years, shape memory alloys (SMAs) attracted wide attentions in the field of seismic control problem (Carreras *et al.* 2011, Casciati and Faravelli 2009, Casciati *et al.* 2017, Casciati and Marzi 2010, Fang *et al.* 2014, Liu *et al*. 2011, Torra *et al*. 2014, Zhu and Zhang 2008). SMAs are a class of metal alloys which show temperature-dependent cyclic behaviors. Above the austenite finish temperature limit, SMAs exhibited superelastic behavior, which is able to recover large deformation and to dissipate input energy simultaneously. Compared with NiTi SMAs, copper-based SMAs maintain superior superelastic performance in a very wide temperature range. The potential of using SMAs in seismic applications can be traced back to the study (Graesser and Cozzarelli 1991), which well presented the advantages and constitutive model for SMAs. Since then, various types of SMA-based dampers were proposed to reduce excessive seismic demands for seismically resistant structures (Song 2006). In terms of bridges, SMA-based dampers were found effective to control relative displacement between decks and piers (Zhu and Qiu 2014) and to avoid unseating risk of bridge decks (Andrawes and DesRoches 2005). For building structures, installment of SMA dampers not only well controlled displacement and acceleration, but also noticeably mitigated residual deformation (McCormick *et al.* 2007, Qiu and Zhu 2017, Qiu *et al*. 2018). At present, utilizing the temperature sensitivity of SMA, Faroughi (2015) and Santos (2018) developed SMA-based active dampers to intelligently reduce vibration of structure. Lobo (2015) and Huang (2018) analyzed the performance of SMA-based semi-active dampers, which can adjust the stiffness of SMA in real time so as to provide comparable vibration control capacities for a wider frequency range and even behave in a more effective manner. Although SMA dampers have been utilized to mitigate seismic responses for a variety of structures, the study of using SMA dampers in transmission tower-line systems can be rarely found.

Therefore, this paper proposed an innovative SMA-TMD for transmission tower-line systems to reduce seismic demands. In particular, considering the tower-line systems are exposed to environment with severe temperature change, which leads to discernible variation of the dynamic characteristics of both the system and the nonlinear properties of SMA-TMD, this study firstly assessed the seismic control effect of the proposed SMA-TMD at room temperature and then paid focus on the temperature effect. In doing so, three-dimensional finite element models (FEMs) of the transmission tower-line system and SMA-TMD were built in numerical software ANSYS, and then intensive parametric analyses on frequency ratio of TMD and seismic intensity of earthquakes were carried out. In this temperature effect analysis, the considered temperature is from -40 to 40℃, and the case of 20℃ is defined to be the reference case.

2. Tower-line system

2.1 Finite element model

The numerical model of currently transmission tower is based the SZ21 type transmission tower in the Northeast China. The parameters can be found in reference (Tian and Rong 2017), and the performance indices of the transmission lines are listed in Table 1. The towers were built in ANSYS 14.5 (ANSYS 2012). Major members were simulated by element Beam 188, and the transmission lines and insulators were simulated by element Link 10. The main member and diagonal member of the transmission tower are made of Q345 and Q235 steel with the nominal yield strength of 310 MPa and 210 MPa, respectively. The elastic modulus of steel is given as 206 GPa. Pinned connections were built between transmission lines and towers. The tower was fixed at the base. Fig. 1 shows the FEM model of the transmission tower-line system. A total of two spans with a span width of 400 m are shown for demonstration. Each transmission line is modeled with 100 truss elements that account for the geometric nonlinearity, and elastic tension-only material is adopted for the transmission lines. The initial axial force and large deformation effect of the transmission line are considered. The transmission lines are subjected to vertical uniformly distributed gravity loads and form catenary shape. The longitudinal direction, i.e. X direction, is defined to be in parallel with the transmission lines, and the lateral direction, i.e., Y direction, is defined to be in perpendicular to the transmission lines.

The transient dynamic analysis was conducted in ANSYS to obtain the seismic responses of the transmission tower line system. The Newmark integration algorithm is used for time-history analysis of the system. To achieve required accuracy, the Full solution method is adopted. The constraint in earthquake excitation direction is released at

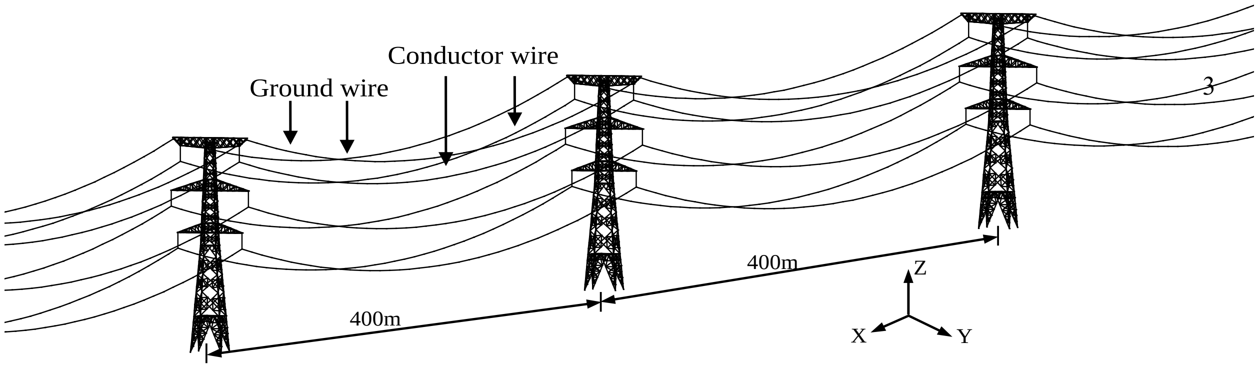

Fig. 1 FEM of transmission tower-line system

the bottom of the transmission tower, and the constraints of the other five degree-of-freedoms are restricted. The earthquake ground motion is imposed to the tower-line system by reading the time history of ground displacement. For the purpose of fully evaluating the performance of SMA-TMD, time history responses of displacement and acceleration at the tower top, that refer to the highest seismic responses, are extracted. It is noted that, upon large earthquakes, the steel components of the transmission tower may lose capacity due to buckling behavior, which will lead to collapse of the system. Further study is needed and will be conducted in future.

2.2 Temperature-dependent frequency of tower-line system

The sag of transmission lines directly determines the tension state of the transmission lines, and is closely related to the stiffness of the tower-line system and the dynamic characteristic of the entire system. The study (Moore and Grace 2000) found that the degree of sag is positively related to the ambient temperature. The total strain of transmission lines includes the elastic strain and thermal strain. Assuming the manufacturing length of transmission lines are constant, the temperature-dependent horizontal stress in transmission lines can be calculated by the state equation of sag (Zhao 2001)

$$\sigma_m - \frac{\gamma_m^2 l^2 E}{24\sigma_m^2} = \sigma - \frac{\gamma^2 l^2 E}{24\sigma^2} - \alpha E(t_m - t) \quad (1)$$

$$\gamma = \frac{9.8p}{A} \quad (2)$$

The maximum sag corresponding to equal hanging height, f, is given by

$$f = \frac{\gamma l^2}{8\sigma} \quad (3)$$

where σ_m, γ_m, and t_m are the horizontal stress, load ratio and temperature of the transmission lines under known state; whereas σ, γ, and t are the corresponding parameters of the transmission lines under unknown state; E is the equivalent elastic modulus of transmission lines; α is the coefficient of linear expansion of transmission lines; P and A are the mass per unit length and cross-sectional area of the transmission lines, respectively.

The temperature used in design procedure and assumed during normal operation is usually 20℃, which corresponds to stresses of 51.8 and 75.6 MPa generated in the lowest points of conductor lines and ground wires, respectively. According to Eq. (3), the maximum sags of both lines and ground wires are 12 m. Based on the results associated with temperature of 20℃, the horizontal stress in transmission lines and the corresponding sag in temperature range of -40 to 40 ℃ with an interval of 10℃ are shown in Figs. 2 and 3, respectively. It is shown that the horizontal stress in transmission lines constantly increases with the decrease of temperature, whereas the maximum sag is reduced when the temperature is decreased. The variation trends of conductor wire and ground wire are nearly identical. Fig. 3 also indicates the maximum sag of conductor wire is sensitive to temperature change, compared to that of ground wire, but they are exactly the same at the temperature of 20℃. It is noted that the considered temperature range is determined based on the possible operation environment of tower-line system.

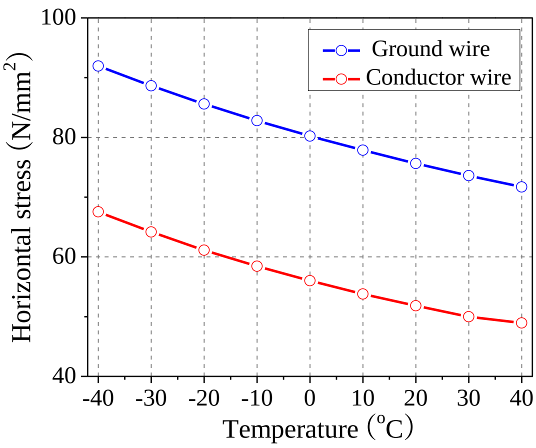

Fig. 2 Horizontal stress in transmission lines

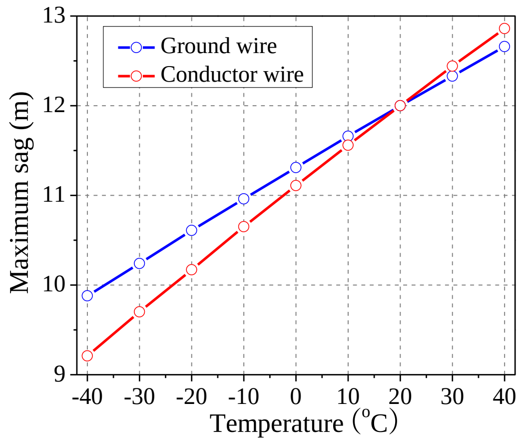

Fig. 3 Maximum sag

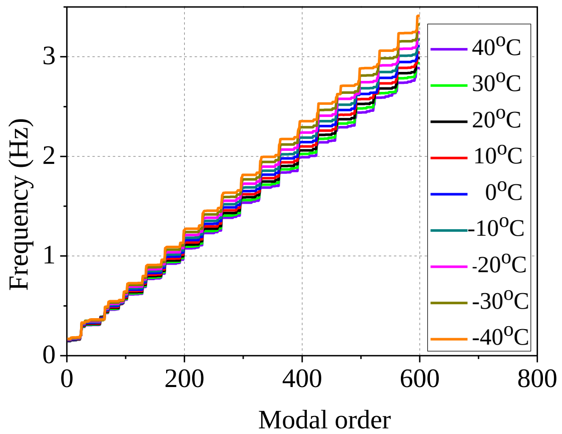

Fig. 4 Frequencies of the tower-line system at various temperatures

The transmission line is very flexible due to a large span, it is prone to endure nonlinear vibration under external loads. This nonlinearity originates from the geometrical change, which is characterized by large displacement while small strain. As presented in above sections, the transmission lines are sensitive to temperature change. With the decrease of temperature, the sags of transmission lines decrease, which results in the change of the shape. Considering the coupling effect between tower and transmission lines, it will consequently affect the dynamic characteristics of the tower-line system as long as the geometry of transmission line changes. Thus, the dynamic characteristics of the tower-line system are dependent on ambient temperature. Eigenvalue analyses are conducted to quantify the extent of variation. Fig. 4 shows the modal frequencies of the tower-line system in the longitudinal direction at various temperatures. The first several vibration modes of tower-line system are dominated by the vibrations of transmission lines. It is seen that the temperature change slightly affects the frequencies of transmission lines, whereas it noticeably affects the vibration of tower. When temperature decreases, the tension stress of transmission line increases, leading to higher stiffness of the tower-line system. Therefore, the frequencies of the system are increased with the decrease of temperature.

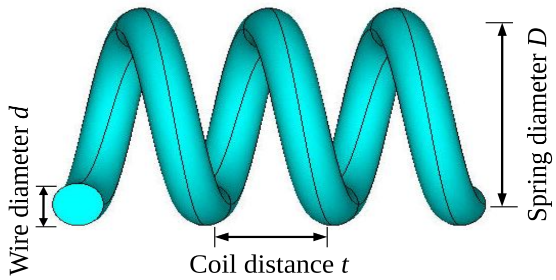

Fig. 5 FEM of helical SMA spring

3. SMA spring

3.1 Simulation of SMA spring

The finite element analysis of SMA spring was conducted in numerical simulation software ANSYS 14.5 (ANSYS 2012). The SOLID185 element was used, and the meshing procedure for the spring was conducted by the mapped method, as shown in Fig. 5. The dimension parameters include wire diameter, *d*, spring diameter, *D* and coil distance, *t*. To generate the cyclic behavior of spring, one end of the specimen was fixed, and the other end was applied with displacement-based loadings. The adopted constitutive model of SMA is given by the software, as shown in Fig. 6. Monocrystalline CuAlBe (M-CuAlBe) is recognized as a promising type of copper-based SMAs for reducing the seismic response of structures, which still has superior superelastic performance in outdoor environment with very low temperature. According to prior test (Qiu and Zhu 2014), with proper training or heating treatment, the M-CuAlBe SMAs are able to exhibit very stable cyclic behavior without strength or damping decay. The mechanical properties of the M-CuAlBe at the room temperature, i.e., 20℃, are extracted from the tests (Qiu and Zhu 2014), as listed in Table 2. It is noted that the full behavior of M-CuAlBe involves two-stage phase transformations, which is much more complicated than the idealized flag-shape behavior, and this cannot be simulated by the software. Therefore, the considered strain is up to 0.14, which refers to the upper limit strain portraying perfect flag-shape behavior. In ANSYS, there are a total of six parameters to describe the hysteretic behavior of SMAs; σ_{Ms} is the onset stress of forward phase transformation; σ_{Mf} is the finish stress of forward phase transformation; σ_{As} is the onset stress of backward phase transformation; σ_{Af} is the finish stress of backward phase transformation; $\bar{\varepsilon}_L$ denotes the maximum recoverable strain,; α measures the difference degree between tension and compression

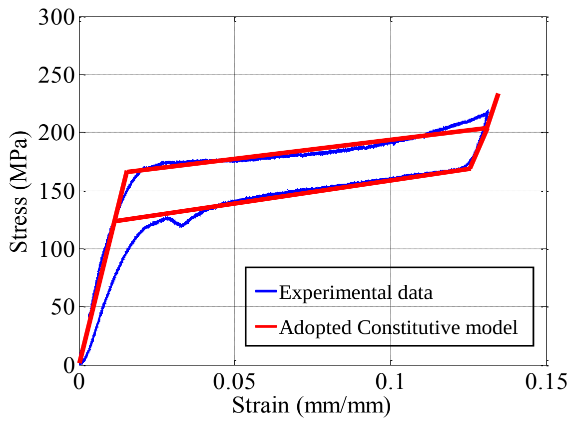

Fig. 6 Constitutive model of SMA

Table 2 Cyclic properties of M-CuAlBe

E	σ_{Ms}	σ_{Mf}	σ_{As}	σ_{Af}	$\bar{\xi}_L$	α
(GPa)	(MPa)	(MPa)	(MPa)	(MPa)	(-)	(MPa)
17	170	200	170	125	0.14	0.17

behavior. In ANSYS, the parameter α characterizes the material response difference in tension and compression. If tensile and compressive behaviors are the same, then α=0. For a uniaxial tension-compression phenomenon, α can be related to the initial value of austenite to martensite phase transformation in tension (σ^{t}_{Ms}) and compression (σ^{c}_{Ms}) as: $\alpha = (\sigma^{c}_{Ms} - \sigma^{t}_{Ms}) / (\sigma^{c}_{Ms} + \sigma^{t}_{Ms})$.

3.2 Temperature effect on SMA

As aforementioned, SMA belongs to temperature-dependent materials, and the cyclic properties of SMA springs will be also affected by temperature change. According to the study (Motahari and Ghassemieh 2007), the stress levels corresponding to the start and finish of phase transformations will be linearly increased with the increase of temperature, whereas the hysteresis shape is unaffected and superelasticity is maintained given the ambient temperature is still above the austenite finish temperature. The relationships between phase transformation stresses and ambient temperature are given as below

$$\sigma_{Ms} = \sigma^{o}_{Ms} + C_M (T - T_o) \tag{4}$$

$$\sigma_{Mf} = \sigma^{o}_{Mf} + C_M (T - T_o) \tag{5}$$

$$\sigma_{As} = \sigma^{o}_{As} + C_A (T - T_o) \tag{6}$$

$$\sigma_{Af} = \sigma^{o}_{Af} + C_A (T - T_o) \tag{7}$$

where T_o and T are the reference temperature and target temperature, respectively. σ^{o}_{Ms}, σ^{o}_{Mf}, σ^{o}_{As} and σ^{o}_{Af} are the phase transformation stresses corresponding to the reference temperature. C_M and C_A are temperature-related parameters, both of which are usually equal to each other (Lagoudas *et al*. 2001).

According to a prior study (Qiu and Zhu 2014), copper-based SMAs have reliable superelasticity in cold-temperature conditions compared with Ni-Ti SMAs to some extent. Therefore, one of the emphases of this study is to preliminarily analyze the applicability of M-CuAlBe to transmission tower-line system at low temperatures. The considered temperatures are from -40 to 40℃ with an increment of 10℃, which are larger than the austenite finish temperature of -91℃. The reference temperature is defined to be T_o=20℃, the parameters C_M = C_A = 1.48 MPa/℃. The phase transformation stresses can be readily calculated by Eqs. (4)-(7). It is noted that the temperature range considered in the test (Qiu and Zhu 2014) is -40 to 20℃, which cannot cover the range of variation of outdoor temperature, but the phase transformation stresses of M-CuAlBe at higher temperatures can be calculated by Eqs. (4)-(7). Therefore, the phase transformation stress corresponding to 30℃ and 40℃ can be reasonably predicted. With the material properties known, the cyclic behaviors of the SMA spring at various temperatures are numerically obtained, as shown in Fig. 7. To make a direct comparison, the applied displacement loads are set to be 0.2 m in all cases. It is seen that the values of elastic stiffness of all springs are constant, which is unaffected by temperature variation. The strength capacity of spring decreases when the temperature is decreasing, which is due to the decreased phase transformation stresses of SMA. It also should be noted that the equivalent damping ratio is raised when the temperature is decreased from -40 to 40℃.

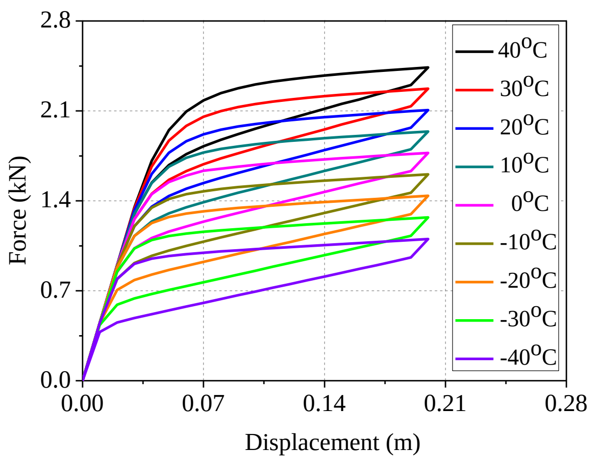

Fig. 7 Cyclic behavior of SMA spring at various temperatures

3.3 Design of SMA spring

To reduce the vibration of the tower-line system, a new TMD system consists of mass and SMA spring is proposed. The SMA-TMD combines the mechanism of vibration reduction of conventional TMD and hysteretic energy dissipation characteristics of SMA spring. A possible configuration of the SMA-TMD is shown in Fig. 8. The SMA-TMD device consists of a stiff box, the mass block, two SMA springs and smooth surface. Since placed on the smooth surface, the restoring force of the mass block is entirely provided by SMA springs. The SMA-TMD is bolted at the top of the tower, and it will be activated in the seismic input direction, as shown in Fig. 8. The SMA-TMD essentially consists of mass and SMA spring. The mass is determined to be 2% of the first modal mass. The SMA spring offers lateral stiffness for the TMD system. It is worth noting the transient stiffness of the SMA-TMD system varies with the nonlinear behavior of SMA spring during earthquakes. In accordance with conventional TMD (Zuo *et al.* 2017), the initial elastic stiffness k_{tmd} of the SMA spring is calculated by

$$k_{tmd} = m\omega^2 \tag{8}$$

An appropriate determination of this parameters leads to success reducing seismic response of transmission tower-line system. This requirement can be achieved by adjusting the natural frequency of SMA-TMD to match the natural frequency of the system. However, when the SMA-TMD is fixed to the system, the natural frequency of the system may change due to the increase of the total mass. Therefore, an optimal coefficient (Den Hartog *et al.* 1985) is introduced to take the mass variation of the system into account, which can be expressed as

$$f_{opt} = \frac{1}{1+\mu_m} \tag{9}$$

According to the principle of structural dynamics, when the natural frequency of TMD is consistent to that of the main structure, TMD will achieve the best control effect. Therefore, the optimal stiffness k_{opt} of SMA-TMD can be expressed as

$$k_{opt} = f_{opt}^2 k_{tmd} \tag{10}$$

where f_{opt} is the optimal frequency of the SMA-TMD, m is the mass of the SMA-TMD and m=316 kg, μ_m is the mass ratio of TMD to controlled mode of transmission tower-line system, ω is the natural frequency in the seismic input direction.

The dimension parameters of spring obey the following relationship

$$d = \sqrt[4]{\frac{8k_{opt}nD^3}{G}} \tag{11}$$

where d and D are wire diameter and spring diameter, respectively; n is coil number; G is the shear modulus of the material, $G = E / 2(1 + \upsilon)$. E and υ are elastic modulus and Poisson ratio of the material, respectively.

Above equations give the 'optimal stiffness' for the SMA-TMD, which are based on the theory for linear TMD. However, for the SMA-TMD, the nonlinear behavior will be activated by seismic force and is critical to the control effect. Besides with the stiffness, the “yield” strength of SMA-TMD requires to be determined. The determined strength of SMA spring is expected to show desirable control effect at the reference temperature upon selected earthquake ground motion record.

To determine the desired strength of SMA spring, a number of combinations of parameters, i.e., d, D and n, are available. This study fixes the coil number of spring to be three, the wire diameter and spring diameter are tuned through parametric analyses. The elastic stiffness of the SMA spring is kept constant, as calculated by Eq. (11).

This paper aims to focus on the temperature effect on the vibration control effect of SMA-TMD on transmission tower-line system subjected to earthquakes. Thus, the representative El Centro seismic wave is selected, although there are many different types of seismic waves with their unique properties. It should be noted that the control effect of TMD is highly dependent on the characteristics of the imposed earthquakes (Matta 2012). Thus, further study should be carried out to quantify the effect of earthquake characteristics on the vibration control effect of SMA-TMD for transmission tower-line systems. The El Centro ground motion record was selected in the design procedure. Considering the seismic intensity of the location site of the adopted tower-line system, and to match the spectral acceleration demand at the fundamental period of the transmission tower-line system, the earthquake ground motion is scaled. Fig. 9 shows the design spectrum and response spectrum of the scaled ground motion agree with each other reasonably well. After adjustment, The PGA is 0.19 g.

Fig. 10 plots the force-displacement relationships for a total of 11 SMA springs. It clearly shows the significant dependence of “yield” strength on the diameter. The larger the diameter is, the higher the strength of the spring will be. Parametric analyses were carried out to assess the seismic control effect of using different SMA springs. Nonlinear time history analyses were conducted for the tower-line system under the scaled ground motion record. Fig. 11 presents the reduction ratios of displacement and acceleration as a function of spring diameter, D. It is found that the reduction ratio initially increased with the increase of D, whereas it peaks when D is approximately equal to 0.05 m, and then the reduction ratio decreases. Therefore, the spring diameter, D, is defined to be 0.05 m. With n and D determined, the other parameters, including d and t are calculated to be 0.012 m and 0.02 m, respectively. Such SMA spring will be used in the following seismic control analyses.

7

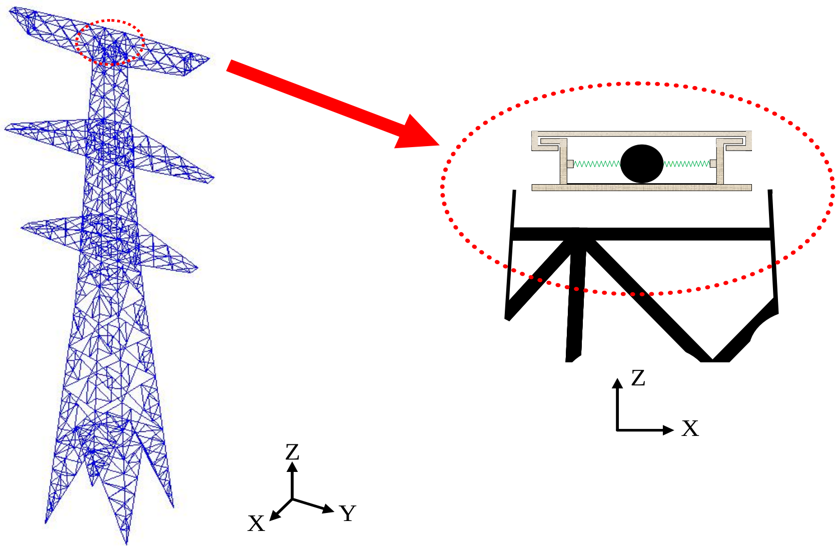

Fig. 8 Location of the proposed SMA-TMD

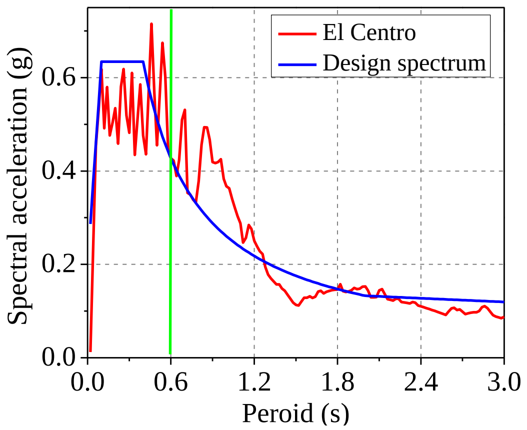

Fig. 9 Design spectrum and response spectrum of El Centro ground motion record

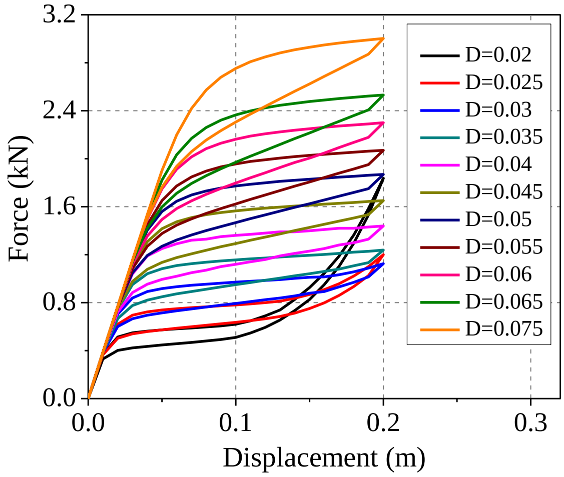

Fig.10 Force-deformation relationships of SMA-spring with various diameter

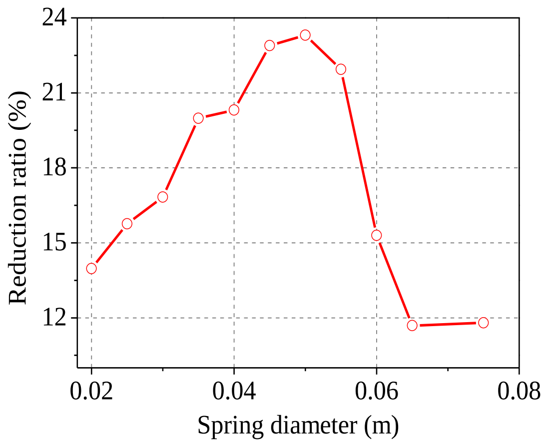

(a) Displacement

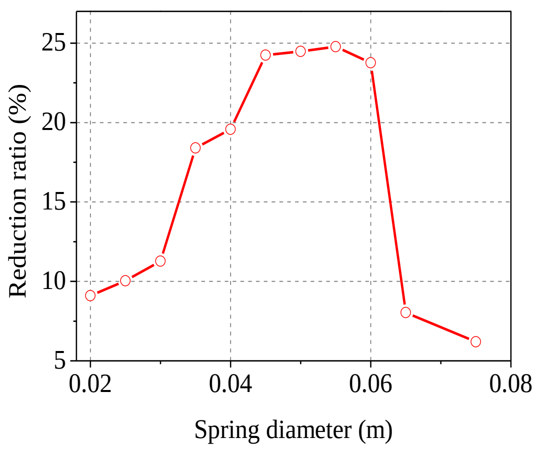

(b) Acceleration

Fig. 11 Reduction ratios of seismic performance indices by using SMA springs with different spring diameters

4. Temperature variation on seismic control effect

To assess how temperature variation affects the seismic control effect of using SMA-TMD in transmission tower-line system, the scaled ground motion record El Centro is input into the system, at temperatures from -40 to 40℃ with an interval of 10℃. The interested seismic performance indices include peak displacement and acceleration at the tower top, and height-wise deformation of the tower. Reduction ratio, η, is introduced to quantify the control effect, defined as below

$$\eta = \frac{R_0 - R_1}{R_0} \times 100\% \tag{12}$$

where R_0 and R_1 are the maximum seismic responses or the root mean square (RMS) of the tower-line system equipped without and with SMA –TMD, respectively.

Fig. 12 presents the seismic responses of the tower-line system with and without control, in terms of time history responses of displacement and acceleration at the tower top and the deformation along the tower height. It is seen that the SMA-TMD successfully reduced seismic demands for the system, regardless of temperature variation. The vibrations of tower are well controlled throughout the height. Due to the temperature-dependence characteristic of SMA spring, the control effect varies with temperature variation, and shows a consistent trend, as shown in Fig. 13. When temperature is decreased from 30 to -40℃, the reduction ratios of displacement and acceleration are decreased from 23.6% and 25.4% to 14.1% and 13.1%, respectively. Similar trend can be found in the values of root mean square (RMS). On average, the reduction ratio decreases 1.5% as the temperature is decreased by 10℃. It should be noted that the vibration reduction effect of SMA-TMD is slightly weakened at the temperature of 40℃. Although the "yield" stress of M-CuAlBe significantly increases at 40℃, the SMA-TMD may be slightly "off-tuning" due to temperature variation, resulting in a drop in the reduction ratios curve. The seismic behavior of SMA springs is assessed to address the temperature effect. Fig. 14 plots the cyclic behavior of the SMA spring at various temperatures, it shows the peak deformation of the SMA spring decreases with the decrease of temperature. In low-temperature environment, the SMA spring gained increased damping, as aforementioned in Section 3.2, which actually suppressed the vibration of the SMA spring, whereas sacrificed the control effect of the tower-line system to a certain degree as a result. The effect of using additional damping in the TMD system can be also found in prior studies (Soong 2014). Due to temperature variations, the fundamental frequency of the tower-line system changes. For linear TMD, the control effect is probably deteriorated and it may even amplify the seismic response of the protected system. However, due to the properly tuned nonlinear behavior, the SMA-TMD offered robustness seismic control effect in a wide frequency range due to temperature change.

5. Parametric analyses

Due to the uncertainty nature of earthquakes, the seismic control effect of SMA-TMD is also examined by varying frequency ratio of TMD and seismic intensity of earthquake at various temperatures. Unless mentioned otherwise, the seismic intensity is 0.19 g, the mass ratio is 0.02, and the frequency ratio is determined as before. The interested seismic response indices include peak displacement and acceleration at tower top.

Fig. 15 presents the effect of varying frequency ratio on the seismic reductions of displacement and acceleration at various temperatures. The optimal frequency ratio is significantly dependent on the ambient temperature, as can be found in both displacement and acceleration performance. It can be seen from Fig. 15 that when the frequency ratios increase from 0.8 to 1.2, the reduction ratios of SMA-TMD all show a trend of increasing first and then decreasing at different temperature. This is because the reduction ratio is affected by the relationship between the natural frequency of SMA-TMD and natural frequency of tower-line system. When the temperature is decreased,

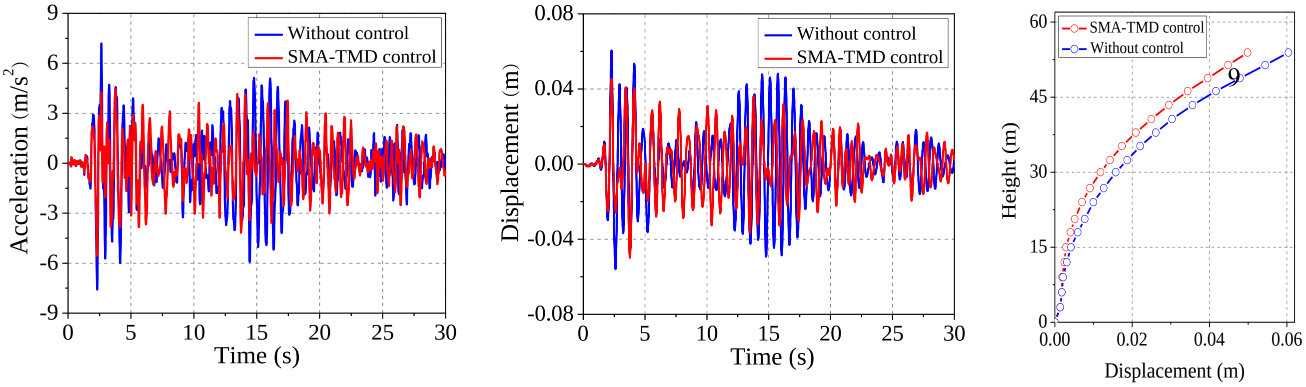

(a) T = 40℃

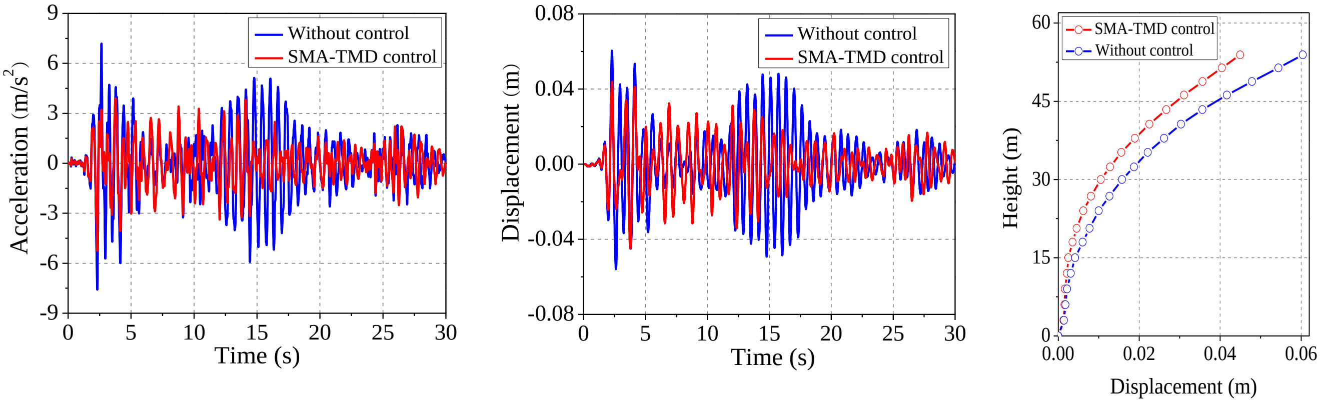

(b) T = 30℃

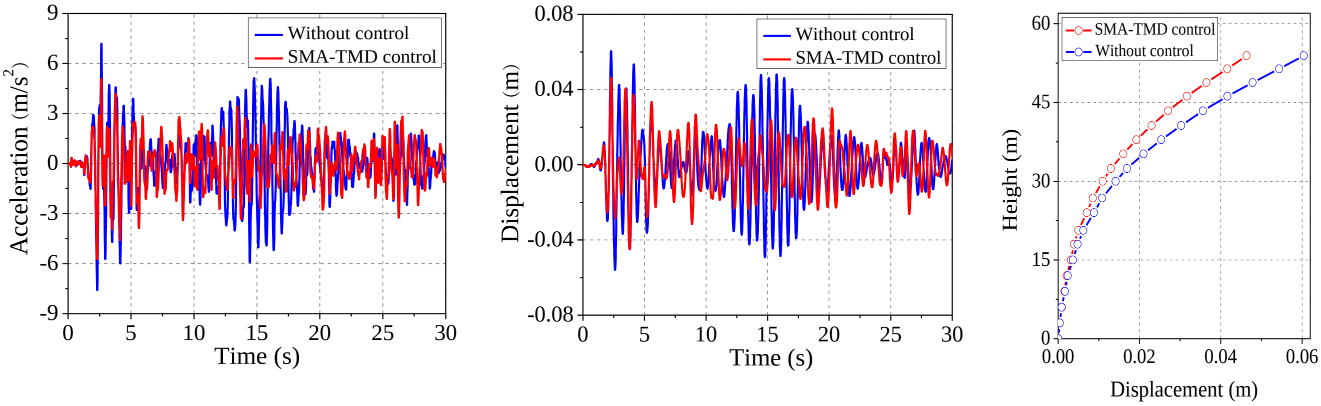

(c) T = 20℃

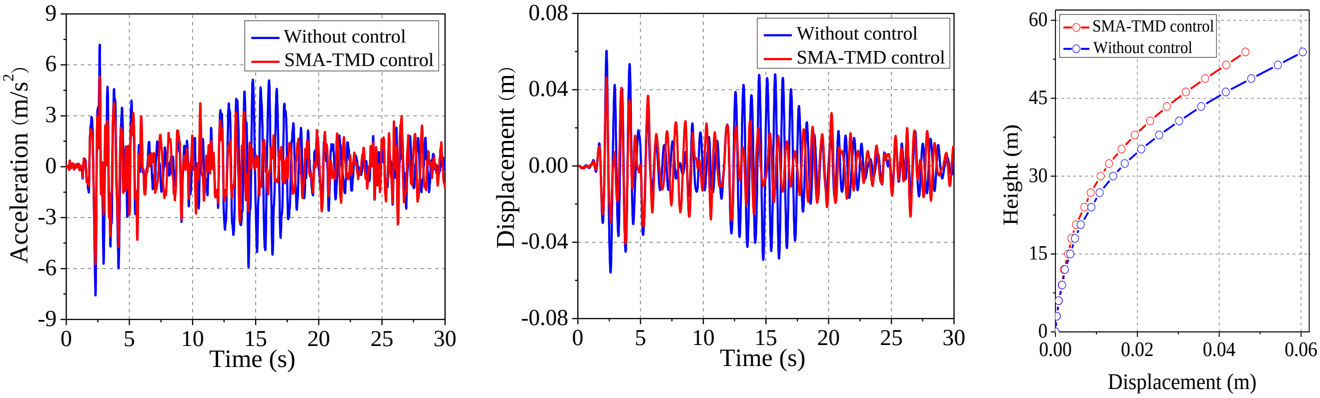

(d) T = 10℃

Continued-

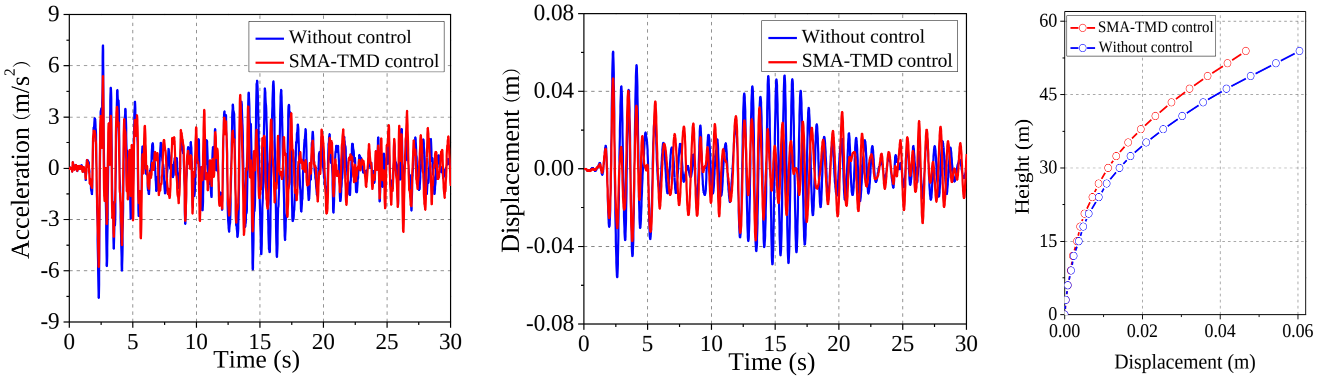

(e) T = 0℃

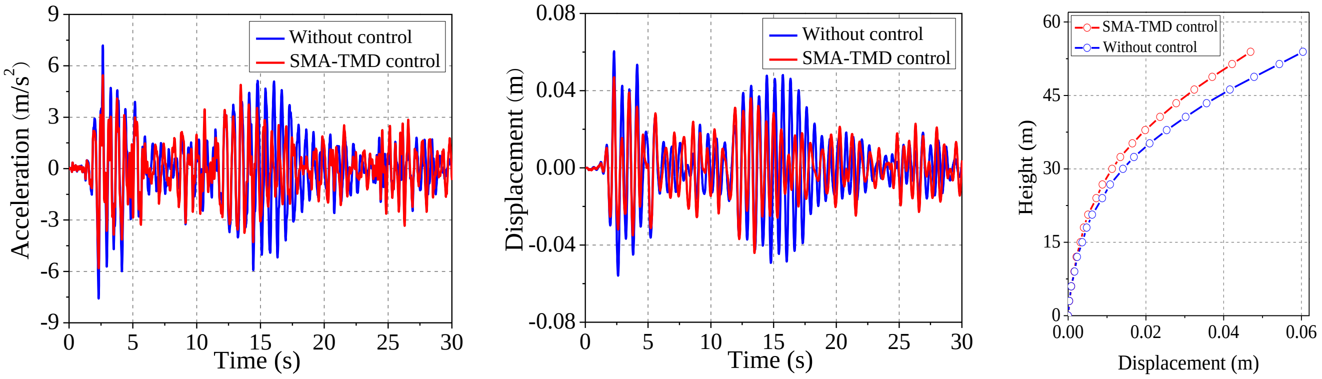

(f) T = -10℃

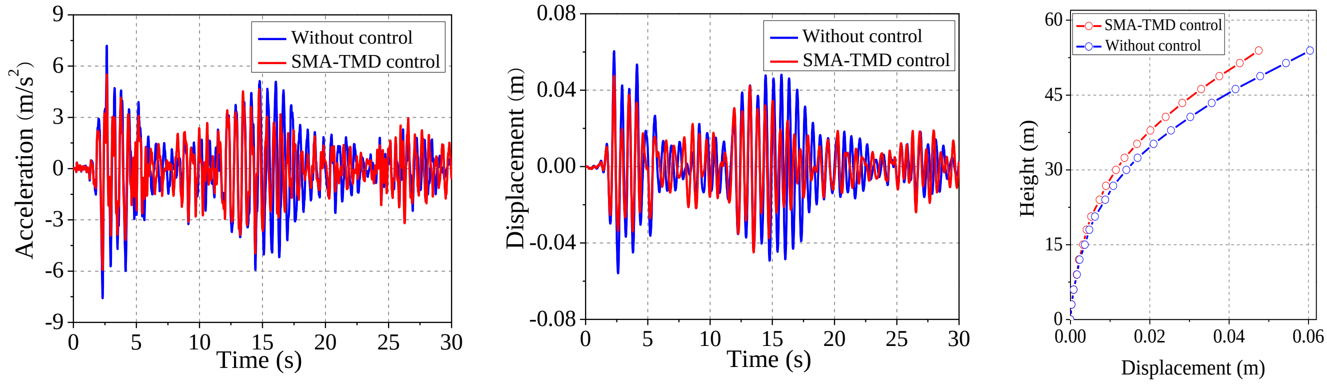

(g) T = -20℃

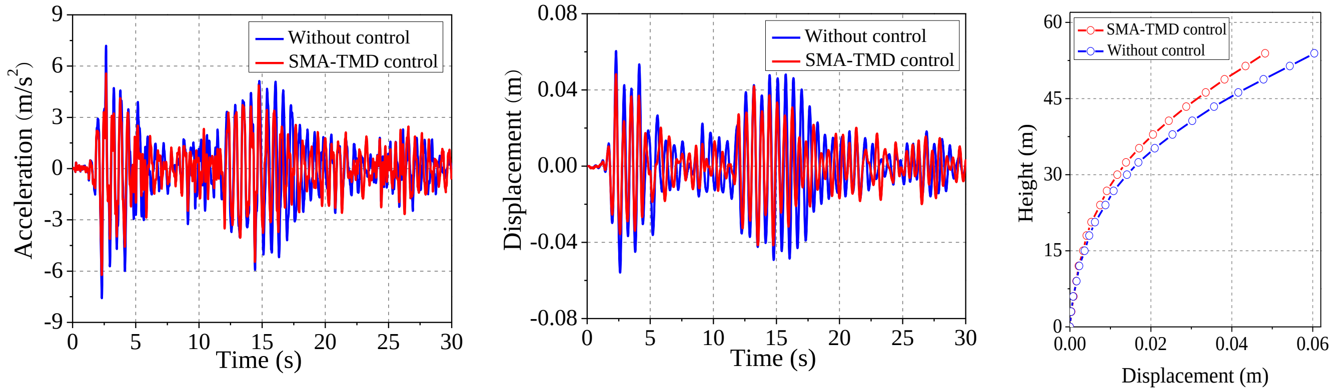

(h) T = -30℃

Continued-

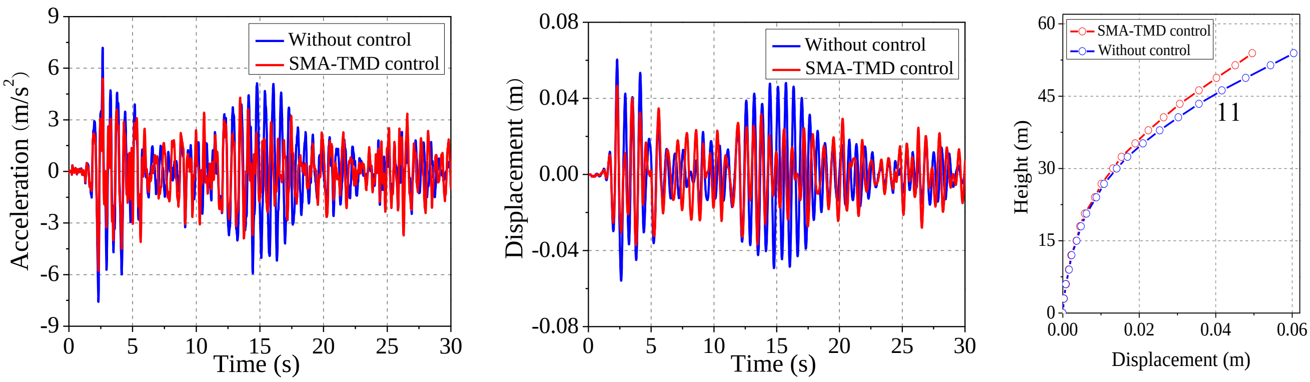

(i) T = -40℃

Fig. 12 Time history responses of tower at various temperatures

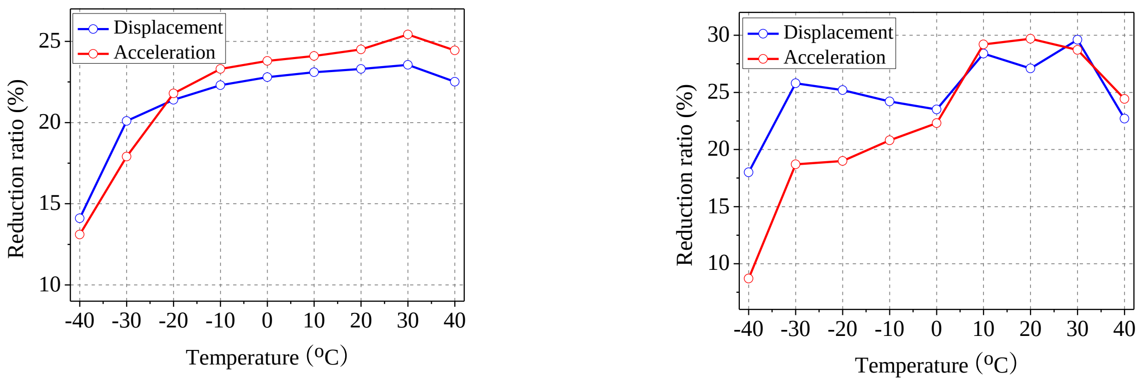

(a) Peak reduction ratio

(b) RMS reduction ratio

Fig. 13 Vibration reduction ratio at different temperatures

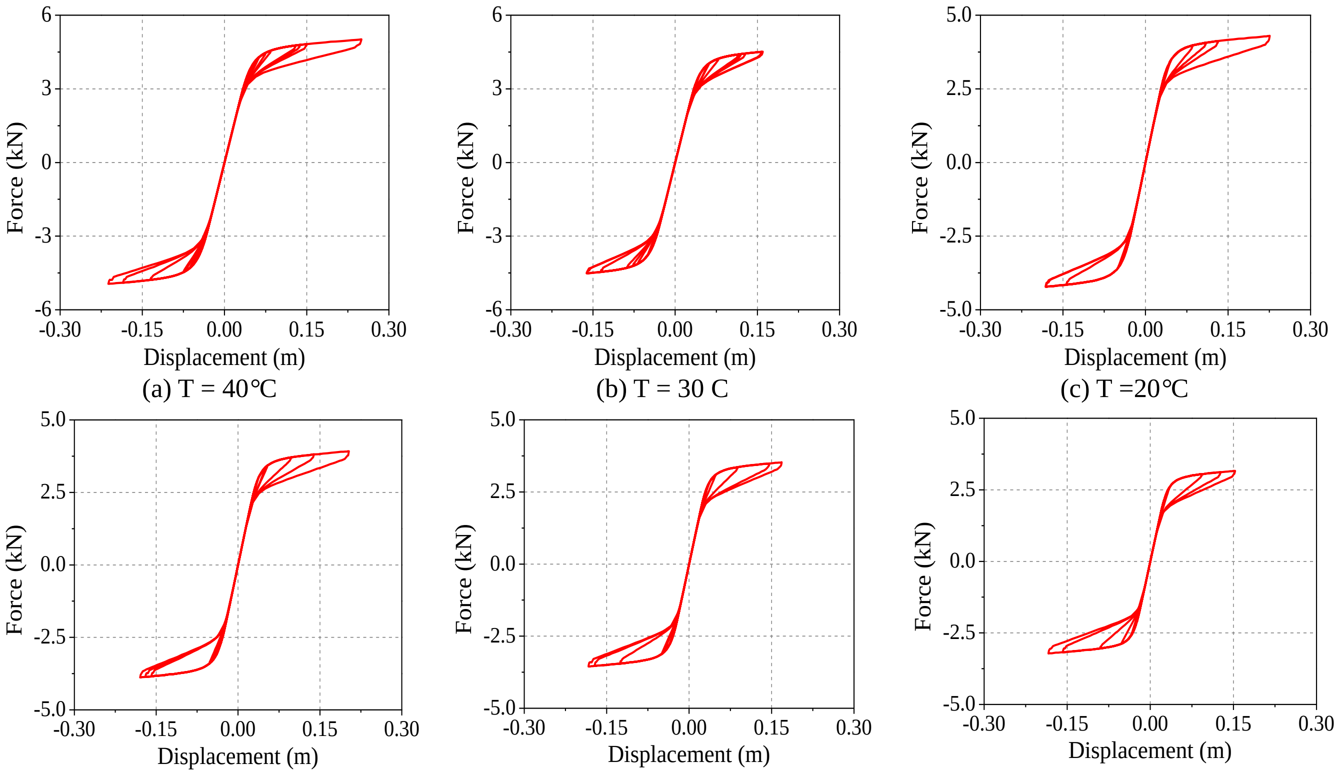

(a) T = 40℃

(b) T = 30 C

(c) T =20℃

(d) T = 10℃

(e) T = 0℃

(f) T = -10℃

Continued-

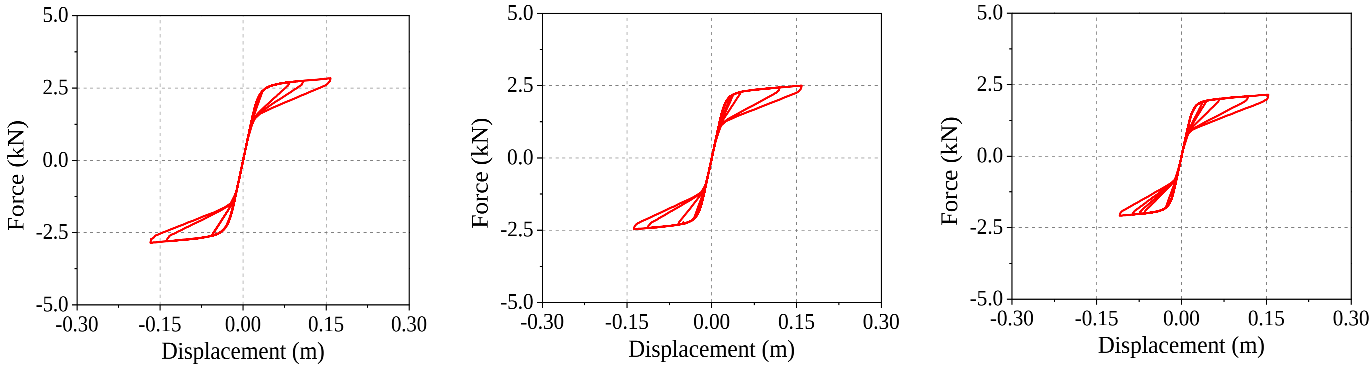

(a) T = -20℃ (b) T = -30 C (c) T -40℃

Fig. 14 Hysteresis curve of SMA spring at different temperatures

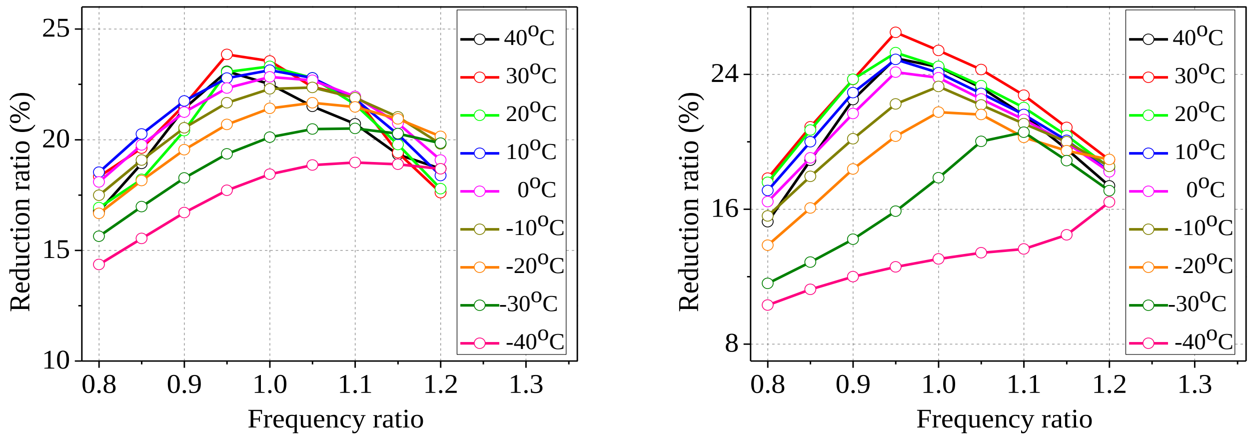

(a) Displacement (b) Acceleration

Fig. 15 Vibration reduction ratio of the SMA-TMD with different frequency ratios

the optimal frequency ratio approximately increases from 0.95 to 1.1. This is because low temperature increased the stiffness of the tower-line system, and thus increased the fundamental frequency of the system. In particular, at temperature of -40℃, the optimal frequency ratio is found over 1.1, which also explained the lowest reduction ratio occurred in this case. Although the frequency ratio is varied in a wide range from 0.8 to 1.2, the reduction ratios of displacement and acceleration are always larger than 14% and 10%, respectively, under all temperatures.

5.2 Seismic intensity of earthquake

The effect of seismic intensity of earthquake is analyzed by subjecting the tower-line system to two levels of earthquakes. The ground motion record, shown in Fig. 9, refers to medium earthquake and it was scaled up by twice to represent large earthquake, according to Chinese National Standard (2015). In this paper, the medium earthquake is determined according to the basic seismic intensity of the location site of the adopted tower-line system. Peak ground acceleration (PGA) of large earthquake is 1.6~2.3 times that of medium earthquake according to *Seismic Ground Motion Parameters Zonation Map of China* (2015). The PGAs of medium and large earthquakes are 0.19 and 0.38 g, respectively. Fig. 16 plots the reduction ratios of displacement and acceleration at various temperatures upon two levels of earthquakes. When the earthquakes are amplified, the trend of temperature variation on seismic control effect of SMA-TMD is comparable in terms of displacement, but the reduction of acceleration is relatively more stable in the case of large earthquake. It is also interesting to note that the reduction ratio is reduced when the earthquake is intensified.

6. Conclusions

This paper examined the effect of temperature variation on the seismic behavior of transmission tower-line system equipped with SMA-TMD. The numerical model of the tower-line system and SMA-TMD were built in ANSYS. To this nonlinear TMD, the stiffness and “yield” strength were well tuned before temperature effect analysis. The considered temperature range is from -40 to 40℃. The interested seismic performance indices include the peak displacement and acceleration at the tower top and deformation along tower height. Parametric analyses on frequency ratio of TMD and seismic intensity of earthquake were also conducted. Following conclusions are obtained:

- Considering the nonlinearity of SMA constitutive model, it is necessary to properly select the dimensions of SMA-TMD before formal applications.
- There are significant influences of temperature variation on both the dynamic responses of the transmission tower-line system and nonlinear behavior of SMA-TMD.
- In the considered temperature range, the SMA-TMD always shows desirable seismic control effect for the tower-line system, which provides a guidance for the engineering applications.
- Through the analysis of frequency ratio and seismic intensity, SMA-TMD still presents stable performance in the case of uncertainty of ambient condition.

According to the study, the vibration reduction ratio is larger than 10% in most cases, which implies the robustness of the SMA-TMD is reasonably good in this study. Moreover, the comparisons between SMA-TMD and conventional TMD has shown the SMA-TMD has an improved robustness. However, the ‘off-tuning” effect caused by the working conditions changes e.g. working temperature changes could lead to great excessive vibration. In terms of how to improve the vibration control robustness, it is actually a common challenge to many seismic vibration control problems. Besides, the SMA-TMD exhibits severe nonlinearity, which makes it even more difficult to obtain an analytical solution to this problem.

Acknowledgements

This research was supported by the National Natural Science Foundation of China (No.: 51808317, 51778347 and 51578325), the Young Scholars Program of Shandong University (No.: 2017WLJH33), and the Natural Science Foundation of Shandong Province, China (No.: ZR2017BEE004). However, any opinions, findings, conclusions and recommendations presented in this paper are those of the authors and do not necessarily reflect the views of the sponsors. Finally yet importantly, the authors wish to thank the anonymous reviewers for their careful evaluations and insightful comments that helped improve the paper.

References

Andrawes, B. and DesRoches, R. (2005), “Unseating prevention for multiple frame bridges using superelastic devices”, *Smart Mater. Struct.*, **14**(3), S60.

ANSYS, Inc. (2012), ANSYS structure Analysis Guide Release 14.5. SAP, IP Inc.

Carreras, G., Casciati, F., Casciati, S., Isalgue, A., Marzi, A. and Torra, V. (2011), “Fatigue laboratory tests toward the design of SMA portico-braces”, *Smart Struct. Syst.*, **7**(1), 41-57. http://dx.doi.org/10.12989/sss.2011.7.1.041.

Casciati, F. and Faravelli, L. (2009), “A passive control device with SMA components from the prototype to the model”, *Struct. Control. Health. Monit*, **16**(7-8), 751-765. https://doi.org/10.1002/stc.328.

Casciati, S., Faravelli, L. and Vece, M. (2017), “Investigation on the fatigue performance of Ni-Ti thin wires”, *Struct. Control Health Monit.*, **24**(1) e1855. doi: 10.1002/stc.1855. https://doi.org/10.1002/stc.1855.

Casciati, S. and Marzi, A. (2010), “Experimental studies on the fatigue life of shape memory alloy bars”, *Smart Struct. Syst.*, **6**(1), 73-85. http://dx.doi.org/10.12989/sss.2010.6.1.073.

Chen, B., Weng, S. and Zhi, L. (2017), “Response control of a large transmission tower-line system under seismic excitations using friction dampers”, *Adv. Struct. Eng.*, **20**(8), 1155-1173. https://doi.org/10.1177/1369433216679999.

Chinese National Standard, (2015), Seismic Ground Motion Parameters Zonation Map of China, *Chinese National Standard*, Beijing, China, 2015, in Chinese.

Den Hartog, J.P. (1985), “Mechanical vibrations”, Courier Corporation.

Fang, C., Yam, M.C.H., Lam, A.C.C. and Xie, L.K. (2014), “Cyclic performance of extended end-plate connections equipped with shape memory alloy bolts”, *J. Constr. Steel. Res.*, **94**, 122-136. https://doi.org/10.1016/j.jcsr.2013.11.008.

Faroughi, S. (2015), “Adaptive tunable vibration absorber using shape memory alloy”, *Mech. Adv. Compos. Struct.*, **2**(1), 55-60. DOI: 10.22075/MACS.2015.332.

Graesser, E.J. and Cozzarelli, F.A. (1991), “Shape-memory alloys as new materials for aseismic isolation”, *J. Eng. Mech.*, **117**(11), 2590-2608. https://doi.org/10.1061/(ASCE)0733-9399(1991)117:11(2590).

Hall, J.F., Holmes, W.T. and Somers, P. (1994), “Northridge earthquake of January 17, 1994”, Earthquake Engineering Research Institute, California, USA.

Huang, H. and Chang, W.S. (2018), “Application of pre-stressed SMA-based tuned mass damper to a timber floor system”, *Eng. Struct.*, **167**, 143-150. https://doi.org/10.1016/j.engstruct.2018.04.011.

Kilroe, N. (2000), “Aerial method to mitigate vibration on transmission towers”, *Proceedings of the Transmission and Distribution Construction, Operation and Live-Line Maintenance.*, Montreal, Canada.

Lagoudas, D.C., Mayes, J.J. and Khan, M.M. (2001), “Simplified shape memory alloy (SMA) material model for vibration isolation”, *Proceedings of the Smart Structures and Materials 2001: Modeling, Signal Processing, and Control in Smart Structures*, Newport Beach, CA, March.

Liu, J.L., Zhu, S., Xu, Y.L. and Zhang, Y.F. (2011), “Displacement-based design approach for highway bridges with SMA isolators”, *Smart Struct. Syst*., **8**(2), 173-190. http://dx.doi.org/10.12989/sss.2011.8.2.173.

Lobo, P.S., Almeida, J. and Guerreiro, L. (2015), “Semi-active damping device based on superelastic shape memory alloys”, *Structures*, **3**, 1-12. https://doi.org/10.1016/j.istruc.2015.06.006.

Matta, E. (2012), “Effectiveness of tuned mass dampers against ground motion pulses”, *J. Struct. Eng. - ASCE*, **139**(2), 188-198. https://doi.org/10.1061/(ASCE)ST.1943-541X.0000629.

McCormick, J., DesRoches, R., Fugazza, D. and Auricchio, F. (2007), “Seismic assessment of concentrically braced steel frames with shape memory alloy braces”, *J. Struct. Eng.*, **133**(6), 862-870. https://doi.org/10.1061/(ASCE)0733-9445(2007)133:6(862).

Miguel, L.F.F., Miguel, L.F.F. and Lopez, R.H. (2016), “Simultaneous optimization of force and placement of friction dampers under seismic loading”, *Eng. Optimiz.*, **48**(4), 582-602. https://doi.org/10.1080/0305215X.2015.1025774.

Moore, P.J. and Grace, D.B. (2000), “Remote sensing of overhead line conductor temperature using an infra-red sensor”, *Proceedings of the 5th International Conference APSCOM 2000*, Hong Kong, October.

Motahari, S.A. and Ghassemieh, M. (2007), "Multilinear one-dimensional shape memory material model for use in structural engineering applications", *Eng. Struct.*, **29**(6), 904-913. https://doi.org/10.1016/j.engstruct.2006.06.007.

Qiu, C. and Zhu, S. (2014), "Characterization of cyclic properties of superelastic monocrystalline Cu–Al–Be SMA wires for seismic applications", *Constr. Build. Mater.*, **72**, 219-230. https://doi.org/10.1016/j.conbuildmat.2014.08.065.

Qiu, C. and Zhu, S. (2017), "Performance-based seismic design of self-centering steel frames with SMA-based braces", *Eng. Struct.*, **130**, 67-82. https://doi.org/10.1016/j.engstruct.2016.09.051.

Qiu, C., Zhang, Y., Li, H., Qu, B., Hou, H. and Tian, L. (2018), "Seismic performance of Concentrically Braced Frames with non-buckling braces: a comparative study", *Eng. Struct.*, **154**, 93-102. https://doi.org/10.1016/j.engstruct.2017.10.075.

Santos, F.A. and Nunes, J. (2018), "Toward an adaptive vibration absorber using shape-memory alloys, for civil engineering applications", *J. Intel. Mat. Syst. Str.*, **29**(5), 729-740. https://doi.org/10.1177/1045389X17721031.

Shuai, X., Jiang, L. and Hou. J. (2014), "Hazard analysis on the characteristics of the M 6.5 Ludian earthquake", *Technology for Earthquake Disaster Prevention*, **9**(3), 340-358. (in Chinese)

Song, G., Ma, N. and Li, H.N. (2006), "Applications of shape memory alloys in civil structures", *Eng. Struct.*, **28**(9), 1266-1274. https://doi.org/10.1016/j.engstruct.2005.12.010.

Soong, T.T. and Constantinou, M.C.(1994), *Passive and Active Structural Vibration Control in Civil Engineering*, Springer-Verlag, New York, NY, USA.

Tian, L., Yu, Q. and Ma, R. (2013), "Study on seismic control of power transmission tower-line coupled system under multicomponent excitations", *Math. Prob. Eng.*, **2013**. http://dx.doi.org/10.1155/2013/829415.

Tian, L., Rong, K. and Zhang, P. (2017), "Vibration control of a power transmission tower with pounding tuned mass damper under multi-component seismic excitations", *Appl. Sciences*, **7**(5), 477. https://doi.org/10.3390/app7050477.

Torra, V., Carreras, G., Casciati, S. and Terriault, P. (2014), "On the NiTi wires in dampers for stayed cables", *Smart Struct. Syst.*, **13**(3), 353-374. http://dx.doi.org/10.12989/sss.2014.13.3.353.

Wu, G., Zhai, C.H. and Li, S. (2011), "Effects of tower-line coupling on seismic vibration control of large crossing transmission tower-line system with TMD", *Adv. Mater. Res.*, **243**, 4005-4008. https://doi.org/10.4028/www.scientific.net/AMR.243-249.4005.

Zhang, P., Song, G. and Li, H. (2012), "Seismic control of power transmission tower using pounding TMD", *J. Eng. Mech.*, **139**(10), 1395-1406. https://doi.org/10.1061/(ASCE)EM.1943-7889.0000576.

Zhao, Y., Shen, C. and Lu, J. (2001), "Calculation of the sagging in overhead insulated cable", *Wire & Cable*, (6), 39-41. (in Chinese)

Zhu, S. and Qiu, C. (2014), "Incremental dynamic analysis of highway bridges with novel shape memory alloy isolators", *Adv. Struct. Eng.*, **17**(3), 429-438. https://doi.org/10.1260/1369-4332.17.3.429.

Zhu, S. and Zhang, Y. (2008), "Seismic analysis of concentrically braced frame systems with self-centering friction damping braces", *J. Struct. Eng.*, **134**(1), 121-131. https://doi.org/10.1061/(ASCE)0733-9445(2008)134:1(121).

Zuo, H., Bi, K. and Hao, H. (2017), "Using multiple tuned mass dampers to control offshore wind turbine vibrations under multiple hazards", *Eng. Struct.*, **141**, 303-315. https://doi.org/10.1016/j.engstruct.2017.03.006.